

# Insights into the Post-Translational Methylation of Arginine from Studies of Guanidinium–Water Nanodroplets

Keri McQuinn, J. Scott McIndoe,\* and Fraser Hof\*[a]

**Abstract:** Highly solvated methylated guanidinium ions ( $[\text{Me}_n\text{Guan}(\text{H}_2\text{O})_m]^+$ ;  $n=0-4$  and  $6$ ;  $m=1->50$ ), which model the various post-translationally methylated states of arginine, were generated in the electrospray ionization (ESI) source of an unmodified commercial tandem mass spectrometer. The dehydration processes of highly solvated  $[\text{Me}_n\text{Guan}(\text{H}_2\text{O})_{21}]^+$  ions were

monitored by using energy-dependent ESI MS. These data, together with supporting calculations, provide a detailed picture of the interplay of methylation

**Keywords:** guanidinium · hydrogen bonds · mass spectrometry · post-translational methylation · solvent effects

and hydration, and both the calculations and the experimental evidence suggest a specific structural basis for the observed effects. The ramifications for biochemical binding events that are controlled by the post-translational methylation of arginine to give dimethylarginines are discussed.

## Introduction

The post-translational methylation of arginine, which is mediated by protein arginine methyltransferases (PRMTs), is important in mediating various biochemical pathways. Type I PRMTs produce asymmetric dimethylarginine (aDMA), whereas type II PRMTs produce symmetric dimethylarginine (sDMA) (Figure 1).<sup>[1]</sup> Monomethylarginine is produced as an intermediate in the synthesis of each form of dimethylarginine, but no selective monomethylase has been identified.<sup>[2]</sup> Arginines are often found at protein–RNA interfaces, and the methylation of arginine can disrupt protein–RNA interactions through steric hindrance or by interrupting hydrogen bonding between the arginine and RNA.<sup>[3]</sup> Methylation also causes arginine to be more hydrophobic, and this aspect of the alteration has been proposed to promote binding with RNA.<sup>[3]</sup>

Arginine methylation is also known to affect protein–protein interactions, and a growing list of reports on arginine

demethylation<sup>[4–6]</sup> have shown that this process is reversible and is used in a variety of ways in cell signaling.<sup>[7]</sup> T cell, cytokine, and nerve growth factor receptors all use arginine methylation for signal transduction,<sup>[1]</sup> and methylation of histones and their coactivators has been shown to regulate transcription.<sup>[1]</sup> Dimethylated arginine is also important in DNA repair; it is believed that MRE11, a protein in the MRE11/RAD50/NBS1 complex that is involved in DNA repair, has an asymmetrically dimethylated arginine that is necessary for its role in regulating DNA damage response.<sup>[8]</sup>

We are interested in the binding changes brought about by arginine methylation. Symmetric and asymmetric dimethylated arginines differ in the way they interact with other proteins. For example, the antibodies SYM10 and SYM11 are specific for sDMA but not aDMA,<sup>[9]</sup> and the Tudor domains of the spinal muscular atrophy gene product

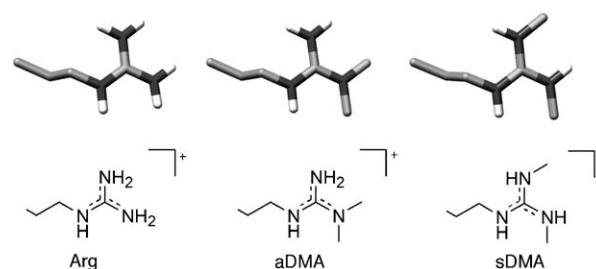


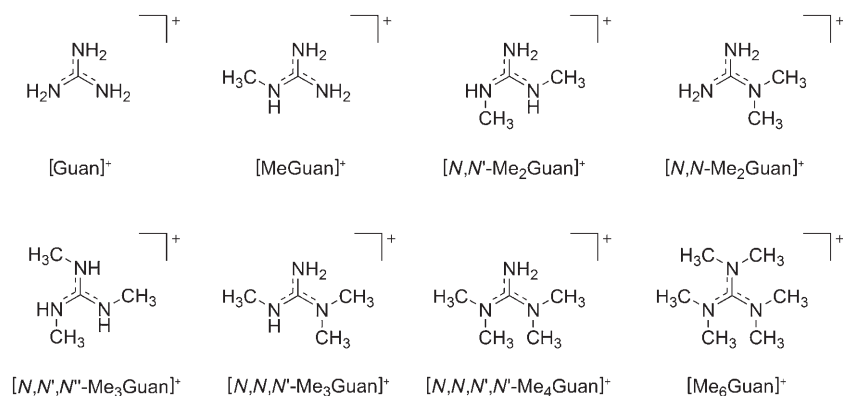
Figure 1. Biologically relevant forms of arginine. Some hydrogen atoms have been omitted for clarity.

[a] K. McQuinn, Prof. J. S. McIndoe, Prof. F. Hof  
Department of Chemistry  
The University of Victoria  
P.O. Box 3065  
Victoria, BC V8W 3V6 (Canada)  
Fax: (+1) 250-721-7147  
E-mail: mcindoe@uvic.ca  
fhof@uvic.ca

Supporting information for this article is available on the WWW under <http://www.chemurj.org/> or from the author.

bind sDMA.<sup>[10]</sup> A study of the folding of  $\beta$ -hairpin model peptides has shown that arginine dimethylation increases the stability of arginine- $\pi$  interactions.<sup>[11]</sup> In this study, both aDMA and sDMA had an identical effect: their incorporation led to a significant entropically driven stabilization of the Arg-Trp cation- $\pi$  interaction that is at the heart of the folded states of the peptides.

The previously mentioned study suggests that the hydrophobic effect is responsible for the methylation-triggered increase in side-chain interactions, and that this may be a common mechanism for triggering many methylation-dependent protein interactions. Methylation of arginine's guanidinium side chain reduces its hydrogen-bonding ability, decreases its charge density, and can force structural changes of the guanidinium core. Each of these factors may interfere with the hydration of the side chain, and therefore, its recognition properties. Guanidinium's role as a common denaturant has been attributed to its relatively weak hydration, its ability to interact with hydrophobic species, and its preference for forming hydrogen bonds to peptides rather than water.<sup>[12,13]</sup> Herein, we examine the effects of side-chain methylation of arginine on hydration by using the novel experimental approach of directly observing the breakdown of highly hydrated guanidinium ions by using energy-dependent electrospray ionization mass spectrometry (EDESI-MS). EDESI-MS is a method of collecting and visualizing collections of data from collision-induced dissociation (CID) experiments.<sup>[14-17]</sup> Similar CID studies have been performed on metal-centered water clusters to probe solvation, fragmentation pathways, and solvent coordination chemistry.<sup>[18,19]</sup> Herein, we used EDESI-MS to observe the loss of water molecules from nanodroplets of water that contained different methylated guanidinium ions. Because our focus is strictly on side-chain methylation, we avoided interference from the arginine backbone atoms by using simple methylated guanidinium ions as models for the various methylated states of the arginine side chain (Scheme 1). Thorough studies of gas-phase guanidine and arginine hydration have been reported elsewhere,<sup>[20-24]</sup> but to the best of our knowledge this is the first study that provides data on the interplay between hydration and side-chain methylation.



Scheme 1. The guanidinium ions studied. [MeGuan]<sup>+</sup>, [N,N'-Me<sub>2</sub>Guan]<sup>+</sup>, [N,N',N''-Me<sub>3</sub>Guan]<sup>+</sup>, and [N,N,N',N''-Me<sub>3</sub>Guan]<sup>+</sup> are models of arginine, methylarginine, sDMA, and aDMA, respectively.

## Experimental Section

**Synthesis:** *N,N,N'*-Trimethylguanidine was synthesized from *S,N*-dimethylthiuronium iodide (Sigma-Aldrich) and aqueous dimethylamine according to a literature method.<sup>[25]</sup> Similarly, *N,N'*-dimethylguanidine was synthesized from aqueous methylamine. Guanidine hydrochloride, methylguanidine hydrochloride, *N,N*-dimethylguanidine sulphate, and *N,N,N',N'*-tetramethylguanidine were purchased from Sigma-Aldrich. Hexamethylguanidine chloride was purchased from Acros Organics and *N,N',N''*-trimethylguanidine was purchased from the Florida Center for Heterocyclic Compounds.

**MS:** All experiments were run on a Micromass Q-ToF micro mass spectrometer in positive ion mode, with a capillary voltage of 2900 V, an ion energy of 1.0 V, a collision cell pressure of 5 p.s.i., and with argon as the collision gas. Aqueous guanidinium solutions with concentrations of between 5 and 10 mM were injected into the mass spectrometer with the cone voltage optimized at 200 V and the source and desolvation temperatures set to 60 and 20 °C, respectively. The solvent flow rates ranged between 50 and 100  $\mu\text{L min}^{-1}$  as the cluster intensities varied. To optimize the formation of methylated guanidinium clusters, the cone gas was turned off and the desolvation gas flow rate was set to 100  $\text{L h}^{-1}$ .

EDESI-MS experiments were carried out by performing MS/MS on the  $[\text{Me}_n\text{Guan}(\text{H}_2\text{O})_{21}]^+$  peak and increasing the collision voltage from 2 to 50 V in one volt increments. Owing to overlap with protonated water-cluster peaks, the  $[\text{MeGuan}]^+$  solutions were run in  $\text{D}_2\text{O}$  to avoid interference. Because  $\text{H}_2\text{O}$  could not be completely removed from the instrument, multiple hydrated species that contained both  $\text{H}_2\text{O}$  and  $\text{D}_2\text{O}$  molecules were observed for each droplet size. For simplicity, the isotopomer  $[\text{MeGuan}(\text{D}_2\text{O})_{21}]^+$  was selected for the MS/MS experiments. Spectra were collected for 30 or 60 s, depending on the cluster intensities, at each collision energy. For the  $[\text{Guan}]^+$ ,  $[\text{N,N',N',N'-Me}_2\text{Guan}]^+$ ,  $[\text{N,N'-Me}_2\text{Guan}]^+$ ,  $[\text{N,N',N'-Me}_3\text{Guan}]^+$ ,  $[\text{N,N',N''-Me}_3\text{Guan}]^+$ , and  $[\text{Me}_6\text{Guan}]^+$  solutions, the mass resolution was set to unit resolution, whereas slightly higher than unit resolution was necessary for  $[\text{MeGuan}]^+$  experiments to ensure that only the peak of interest was mass selected. Automation of the mass spectrometer software (MassLynx) to carry out EDESI-MS experiments (ramping of the collision voltage) was achieved by using the program Autohotkey (freely available from <http://www.autohotkey.com>). EDESI summation spectra were generated by summing the intensities of all 49 spectra (recorded at collision voltages of 2–50 V, in 1 V intervals). The EDESI-MS contour plots were generated such that the contour lines only appeared when the peak intensity had >4% of the intensity of the largest peak in a given spectrum.

**Calculations:** HF 6-31+G\*, density functional B3LYP/6-31G\*\*, B3LYP/6-311+G\*\*, B3LYP/6-311++G\*\*, and Møller-Plesset 6-311++G\*\* equilibrium geometry calculations for each bare guanidinium ion, each guanidinium ion with one water molecule, and a lone water molecule were carried out by using Spartan.<sup>[26]</sup> The water affinity for each guanidinium ion was determined by subtracting the sum of the energies of the individual water molecule and the guanidinium ion from the energy of the complex. Geometries were identified as global minima by manual searching of the limited number of different possible starting geometries.

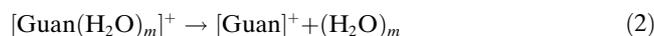
## Results and Discussion

The study of gas-phase water clusters of biologically relevant molecules provides insight into the role of hydration in biomolecular behavior.<sup>[21,27-31]</sup> Water clusters of arginine have been generated by others using IR-

laser ablation techniques<sup>[20]</sup> and nano ESI.<sup>[21]</sup> We found that hyperhydrated guanidinium ions could be more easily prepared by spraying aqueous guanidinium solutions into an unmodified ESI mass spectrometer under cold flooding conditions (high flow rates and cool temperatures; see the Experimental Section for details). These conditions provide ready access to a variety of nanodroplet solvated ions, such as  $\text{H}_3\text{O}^+$ ,  $\text{Ln}^{3+}$ , various substituted anilines,  $\text{Cu}^{2+}$ , and  $\text{Mg}^{2+}$ .<sup>[32–35]</sup> A pick-up technique has also proven reliable for generating many types of multiply charged solvent clusters.<sup>[36,37]</sup> In a similar manner to our previous work, in which we sequentially removed water molecules from triply charged lanthanide-centered water clusters,<sup>[35]</sup> we subjected the methylated guanidinium nanodroplets obtained to EDESI-MS/MS to observe the sequential dehydration of the charged solutes directly, under controlled conditions.

The  $[\text{Me}_n\text{Guan}(\text{H}_2\text{O})_{21}]^+$  cluster of each methylated guanidinium ion (Figure 2) was chosen for the EDESI-MS/MS experiments because these clusters are sufficiently large for

processes for such ion–solvent droplets, that is, the loss of water molecules [Eq. (1)] and the loss of the guanidinium ion [Eq. (2)].



The contour maps for each methylated species (see Figures 2 and 3 and the Supporting Information) generally do not contain naked  $[\text{Guan}]^+$  ions at low collision voltages, which demonstrates that fragmentation through the direct loss of ions from the surface of the water droplets [Eq. (2)] is not a significant contributor under these experimental conditions. However, this process is more significant in the highly methylated species (Figure 3c,d); this is most likely to be a result of the geometry of the cluster formation. As the level of methylation increases and the water–cation interactions weaken, the cation will not necessarily be found at the

center of the water cluster, which makes fragmentation by the route shown in Equation (2) more significant in highly methylated species than in species with less methylation (e.g.,  $[\text{Guan}]^+$ ,  $[\text{MeGuan}]^+$ , and  $[\text{Me}_2\text{Guan}]^+$ ). Note that, in Figure 3c and d, fragmentation through the route shown in Equation (2) appears to be especially significant because the parent ion is observed at low collision voltages. However, if the contour plots are generated with a slightly higher noise cutoff (i.e., 10% of the intensity of the largest peak instead of the 4% cutoff used for the plots in Figures 2 and 3), the contour of the completely desolvated ion  $[\text{M}^+]$  is not present at low collision voltages. Similarly, breaks in the contour lines of the parent ion arise when low-intensity contours

vary near the selected cutoff value. Thus, the water droplets decomposed predominantly through loss of water [Eq. (1)], until low hydration was reached and the two fragmentation processes became more and more similar.

In addition to giving details on the mechanism of droplet fragmentation, the contour maps also revealed subtle differences in the loss of water from different guanidinium ions. At low collision energies and high hydration values, the contour map shows that water molecules were lost at the same rate for both  $[\text{Me}_6\text{Guan}(\text{H}_2\text{O})_m]^+$  (Figure 2b, bottom) and unmethylated  $[\text{Guan}(\text{H}_2\text{O})_m]^+$  (Figure 2a, bottom), and at low collision energies the distribution of water loss for both

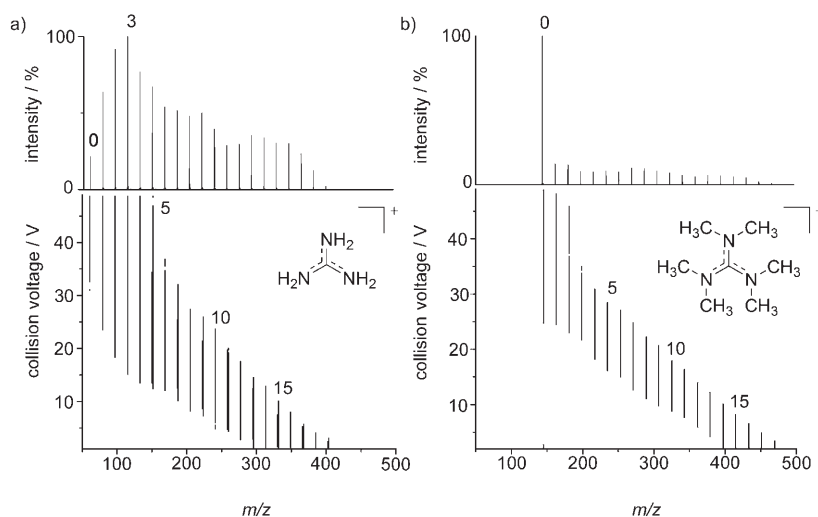


Figure 2. EDESI mass spectra of a)  $[\text{Guan}(\text{H}_2\text{O})_{21}]^+$  and b)  $[\text{Me}_6\text{Guan}(\text{H}_2\text{O})_{21}]^+$ . The bottom plots show the EDESI-MS contour maps; y axis: fragmentation energy and z axis (out of the page): ion intensity. Only contours that had >4% of the intensity of the most intense peak were drawn. The top plots are 2D summation plots, generated by adding all 49 daughter-ion spectra (collision voltages from 2–50 V) that were used to generate the contour maps. The numbers beside individual species represent the number of water molecules in that cluster.

the sequential loss of water outside the first hydration sphere to be observed. The  $[\text{M}(\text{H}_2\text{O})_{21}]^+$  cluster of the *N*-methylguanidinium ( $[\text{MeGuan}]^+$ ) species overlaps with the signals that arise from the protonated water cluster  $[\text{H}(\text{H}_2\text{O})_{26}]^+$ , and therefore,  $[\text{MeGuan}]^+$  was run in  $\text{D}_2\text{O}$  and the  $[\text{MeGuan}(\text{D}_2\text{O})_{21}]^+$  cluster was mass-selected for fragmentation. No significant differences in the resulting EDESI spectra were observed to arise from this isotope substitution.

Figure 2 shows the EDESI-MS summation plots and contour maps for the fragmentation of  $[\text{Guan}(\text{H}_2\text{O})_{21}]^+$  and  $[\text{Me}_6\text{Guan}(\text{H}_2\text{O})_{21}]^+$ . There are two possible fragmentation

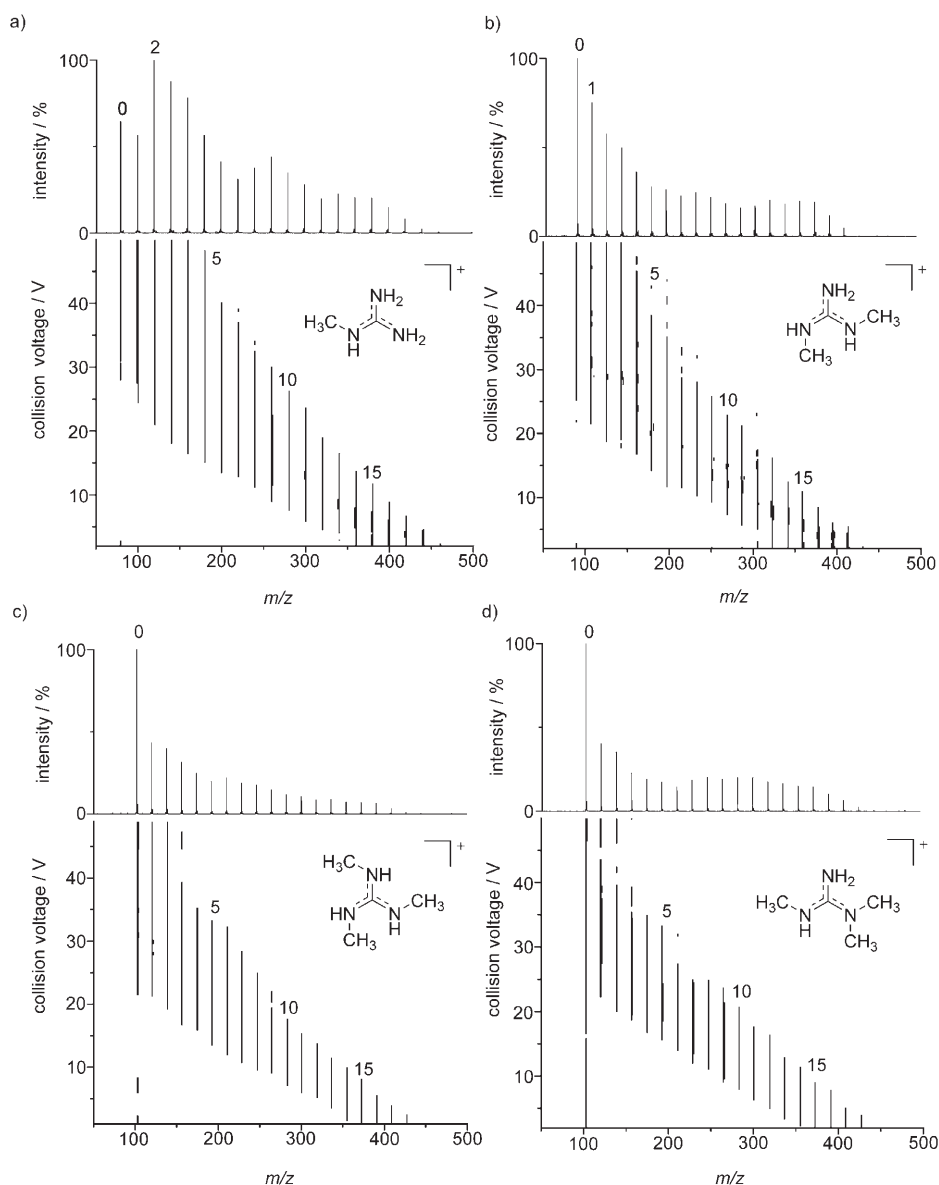


Figure 3. EDESI mass spectra of a)  $[\text{MeGuan}(\text{D}_2\text{O})_{21}]^+$ , b)  $[\text{N},\text{N}'\text{-Me}_2\text{Guan}(\text{H}_2\text{O})_{21}]^+$ , c)  $[\text{N},\text{N}',\text{N}''\text{-Me}_3\text{Guan}(\text{H}_2\text{O})_{21}]^+$ , and d)  $[\text{N},\text{N}',\text{N}''\text{-Me}_3\text{Guan}(\text{H}_2\text{O})_{21}]^+$ . The bottom plots show the EDESI-MS contour maps; y axis: fragmentation energy and z axis (out of the page): ion intensity. Only contours that had  $>4\%$  of the intensity of the most intense peak were drawn. The top plots are 2D summation plots, generated by adding all 49 daughter-ion spectra (collision voltages from 2–50 V) that were used to generate the contour map. The numbers beside individual species represent the number of water molecules in that cluster.

species is identical.<sup>[38]</sup> At lower hydration values (high collision energy), the profile of the contour map for water loss from the  $[\text{Me}_6\text{Guan}(\text{H}_2\text{O})_m]^+$  ion is essentially independent of the hydration value. In contrast, the contour map for  $[\text{Guan}(\text{H}_2\text{O})_m]^+$  shows that water loss becomes more difficult at lower hydration values.

Summation plots, an informative, alternative presentation of these data, are shown above the contour maps in Figures 2 and 3. These plots were generated by summing all daughter-ion data generated throughout the EDESI-MS experiment. They provide an easily accessible way to compare

the dehydration of related species studied under identical conditions. The most intense peaks correspond to species that arise sooner and persist longer during the ramping up of the collision energy that causes dehydration, whereas less intense signals arise from the more fleeting species. The summation plots in Figure 2 reveal large differences between the hydration of  $[\text{Guan}]^+$  and  $[\text{Me}_6\text{Guan}]^+$ . The EDESI-MS summation spectrum of the former shows a low-intensity peak for the completely desolvated ( $m=0$ ) peak; the guanidinium ion is loath to give up its water molecules, and so little of the bare molecular ion was generated during the course of the experiment. The  $[\text{Me}_6\text{Guan}]^+$  spectrum, collected under identical conditions, gives a different picture; the desolvated ( $m=0$ ) peak is dominant, which indicates that the water molecules are easily stripped from this guanidinium ion that is devoid of hydrogen-bond donors.

The spectra for the other methylated guanidinium ions are presented in Figure 3. Across the whole series, it is clear that with increased methylation comes an increased representation of the bare  $[M^+]$  ion in the summed EDESI-MS data. Those members of the series that are models for specific methylated Arg side chains—methylguanidinium as a model for the unmethylated side chain of Arg and both isomeric trime-

thylguanidinium ions as models for the side chains of sDMA and aDMA, see Scheme 1 for structures—are worth closer examination. The summation plot of the Arg model (Figure 3a) is typical of a strongly hydrated species. The intensity of bare  $[\text{MeGuan}]^+$  is low relative to the solvated ion. In contrast, the summation plots of both aDMA and sDMA models (Figure 3c and d) are strikingly similar to that of the completely methylated species  $[\text{Me}_6\text{Guan}]^+$  (Figure 2b), and the intensities of the bare molecular ions are more than double those of any individual hydrated species. From this qualitative view, it is clear that the presence of three or

more methyl groups significantly weakens the hydration of a guanidinium ion. In the context of the physiologically relevant process of Arg side chain methylation, this suggests that dimethylation of Arg to give aDMA or sDMA dramatically decreases the strength of the hydrogen bonds between Arg and water. These gas-phase results correlate well with previously obtained data on the binding of arginine side chains to an aromatic partner in solution. Dimethylation of the side chain improved binding in a manner that was entropically (hydrophobically) driven.<sup>[11]</sup>

We sought a structural understanding of the enthalpic contributions to these methylation effects by using gas-phase calculations of water affinities. The calculated global minimum for each guanidinium ion under study was determined by minimizing a variety of starting conformations. The global-minimum-energy structure for each guanidinium–water structure was then determined in a similar way (Figure 4). Each guanidinium ion remains as planar as possible to maximize conjugation within the central guanidinium core, and methyl groups on adjacent nitrogen atoms choose to avoid mutual steric repulsion whenever possible.

Regardless of method and basis set, the calculated values (Table 1) reveal a key feature of the system. The binding of a single water molecule is slightly weakened upon methylation, even if hydrogen-bonding sites are unaffected and structurally identical (compare, for example,  $[\text{Guan}]^+$ ,  $[\text{MeGuan}]^+$ , and  $[\text{Me}_2\text{Guan}]^+$ ). This can be explained by the reduced charge density, and therefore, weaker hydrogen-bonding ability, of the more highly methylated guanidinium ions.

Methylation of a single NH group obstructs hydrogen-bond donation by that group, but the models in Figure 4 suggest an additional means by which methylation might hinder hydrogen bonding to water. The water molecules bound to the guanidinium ions in Figure 4a–d are held by hydrogen bonds from two adjacent NH groups, whereas the more methylated guanidinium ions in Figure 4e–h lack such pocketlike features and so hold their water molecules with only a single hydrogen bond. Calculations by Soetens et al. on the interaction between unmethylated guanidinium ions and water showed that a water molecule binds more strongly in the pocket between two neighboring NH groups on a guanidinium ion than to a single NH donor.<sup>[40]</sup> Our own calculations reveal the presence of such pockets in guanidinium (three pockets; Figure 4a), methylguanidinium (two pockets; Figure 4b), and both dimethylguanidinium ions (one pocket; Figure 4c,d). Methylated guanidinium ions with three or more methyl groups, which includes the sDMA and aDMA models  $[\text{N,N',N''-Me}_3\text{Guan}]^+$  and  $[\text{N,N,N',N''-Me}_4\text{Guan}]^+$  (Figure 4e,f), do not have this open pocket in their lowest-energy

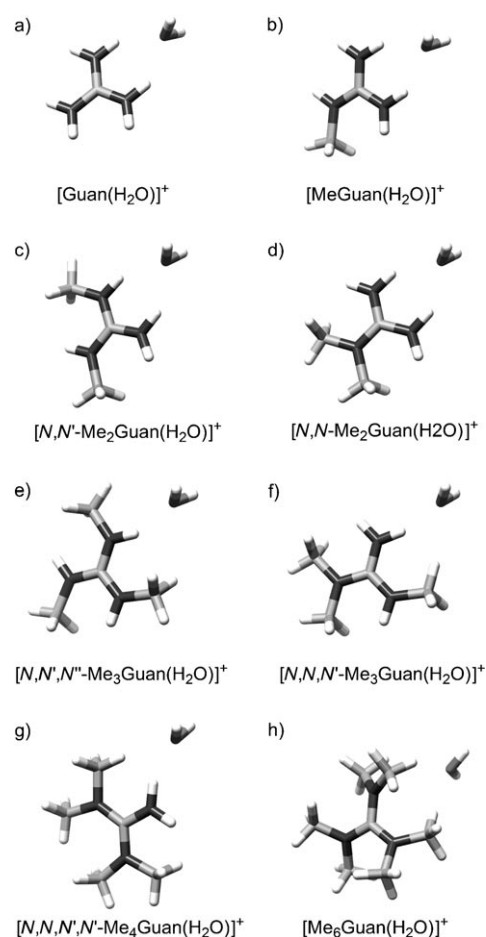


Figure 4. Hydrogen-bonding geometries of each singly hydrated methylated guanidinium (Hartree–Fock (HF) 6-31+G\*). Additional close C...H...O contacts were observed in structures e), f), g), and h).<sup>[39]</sup>

conformations. This suggests that dimethylation of Arg reduces the strength of hydration by lowering the charge density, and may also have a structural ability to decrease the hydrogen-bonding ability of methylated Arg side chain.

These calculations only examine the interaction of each guanidinium ion with a single water molecule, but the experimental EDESI-MS data also reveal evidence for the role of these pockets in controlling the dehydration of guanidinium

Table 1. Calculated water affinities of guanidinium ions.<sup>[a]</sup>

	6-31+G* <sup>[b]</sup>	Water affinity [kcal mol <sup>-1</sup> ]			6-311++G** <sup>[d]</sup>
		B3LYP 6-31G** <sup>[c]</sup>	B3LYP 6-311+G** <sup>[c]</sup>	B3LYP 6-311++G** <sup>[c]</sup>	
$[\text{Guan}]^+$	-17.1	-22.7	-20.6	-22.2	-18.9
$[\text{MeGuan}]^+$	-16.4	-21.0	-17.1	-17.1	-18.2
$[\text{N,N'-Me}_2\text{Guan}]^+$	-17.1	-21.5	-17.5	-17.5	-18.8
$[\text{N,N''-Me}_2\text{Guan}]^+$	-15.7	-20.1	-16.3	-16.2	-17.6
$[\text{N,N',N''-Me}_3\text{Guan}]^+$	-14.2	-17.1	-14.1	-14.0	-16.1
$[\text{N,N',N''-Me}_3\text{Guan}]^+$	-11.8	-16.1	-12.8	-12.7	-13.8
$[\text{N,N,N',N''-Me}_4\text{Guan}]^+$	-8.8	-13.1	-10.2	-10.2	-11.2
$[\text{Me}_6\text{Guan}]^+$	-6.6	-9.9	-7.3	-7.2	n.a. <sup>[e]</sup>

[a] See the Experimental Section for details of the theoretical calculations. [b] HF. [c] DFT. [d] MP2. [e] Did not converge.

ion nanodroplets. The summation plots show that  $[\text{Guan}]^+$  (Figure 2a) and  $[\text{MeGuan}]^+$  (Figure 3a) tenaciously hold on to three and two water molecules, respectively, which corresponds to the number of pockets in each structure. The  $[\text{Me}_2\text{Guan}]^+$  ions (Figure 3b and Figure S1 in the Supporting Information) have a single pocket and appear to retain their last water molecule better than the other, more heavily methylated guanidinium ions, none of which have any double-hydrogen-bonding pockets, and all of which have the water-free molecular ion as the dominant species.

Threshold CID experiments can be carefully performed under single-collision conditions to give quantitative information on ligand binding energies,<sup>[41,42]</sup> and this strategy has also been applied to multiply solvated ions.<sup>[43]</sup> For the sake of simplicity, we have only extracted qualitative information from our experiments, but even these studies allow insight into the processes under study. Figure 5 shows a plot of the

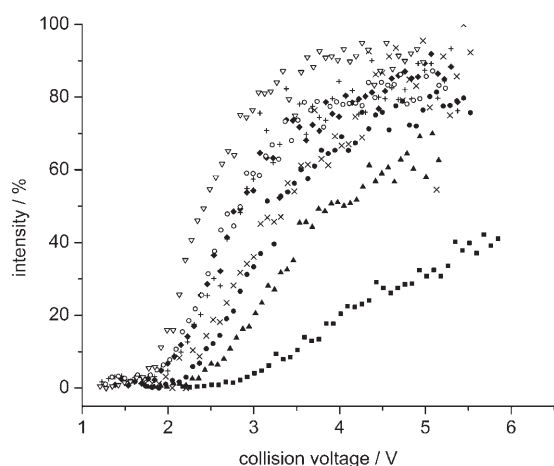


Figure 5. Plot of appearance potential (collision energy corrected for center-of-mass) for the completely desolvated molecular ions ( $M^+$ ) versus the intensities from the EDESI-MS experiments. ■:  $[\text{Guan}]^+$ , ▲:  $[\text{MeGuan}]^+$ , ●:  $[\text{N,N-Me}_2\text{Guan}]^+$ , ×:  $[\text{N,N'-Me}_2\text{Guan}]^+$ , ◆:  $[\text{N,N',N''-Me}_3\text{Guan}]^+$ , +:  $[\text{N,N,N'-Me}_3\text{Guan}]^+$ , ○:  $[\text{N,N,N',N''-Me}_4\text{Guan}]^+$ , and ▽:  $[\text{Me}_6\text{Guan}]^+$ . The ion intensity is plotted as a percentage of the total ion current for all points. The collision voltage ranged from 2 to 70 V. A color version and a normalized plot of this data are presented in the Supporting Information.

appearance potentials for each of the completely desolvated ions. Intensity values were obtained by calculating the percentage of the ion current represented by the final product ion, that is, the completely desolvated guanidinium ion. Generally, increased methylation leads to complete desolvation at a lower collision energy. More specifically, the influence of the pocket structure on the global dehydration processes can also be discerned from the traces, which split cleanly into five groups: three pockets ( $[\text{Guan}]^+$ ), two pockets ( $[\text{MeGuan}]^+$ ), one pocket (the two isomeric  $[\text{Me}_2\text{Guan}]^+$  ions), no pockets (the two isomeric  $[\text{Me}_3\text{Guan}]^+$  ions and  $[\text{Me}_4\text{Guan}]^+$ ), and no pockets and no available N–H bonds ( $[\text{Me}_6\text{Guan}]^+$ ).

Taken together, these data demonstrate the unsurprising result that methylated Arg side chains are more hydrophobic than their unmethylated counterparts, and explain why aDMA and sDMA behaved identically in a prior experimental binding study that did not allow for shape-selective recognition.<sup>[11]</sup> More interestingly, our calculations and experimental data suggest a structural means by which Arg methylation may control the specific number of strongly bound water molecules in the first hydration sphere of the side chain. In nature a single Arg side chain is not modified with more than two methyl groups, although the chemistry to do so could, presumably, have evolved as it did for the exhaustively methylated trimethyllysine side chain.<sup>[44,45]</sup> When considering hydrophobic binding events as important motivators for Arg methylation and demethylation in a variety of biochemical contexts, it is intriguing that the dimethylation of Arg to produce aDMA or sDMA is sufficient to completely remove the pocketlike structures that seem to be required for strong side-chain hydration.

## Conclusion

The study of solution-phase properties by using gas-phase solvent droplets is a well-established method used by physical chemists for over 40 years.<sup>[46]</sup> The enormous popularity of ESI mass spectrometers worldwide, and the ease with which such instruments can produce hyperhydrated ions, means that these ion–water nanodroplets are now accessible to a large and growing number of chemists and biochemists. EDESI-MS is a simple technique that can be performed on common, unmodified, commercially available mass spectrometers with MS/MS capabilities.<sup>[14–16,35,47]</sup> The results reported herein demonstrate that these relatively simple EDESI-MS experiments can quickly provide insightful and relevant information on the hydration of post-translationally methylated arginine side chains. We look forward to applying this technique to the study of other physiologically relevant motifs.

## Acknowledgements

J.S.M. and F.H. both thank the Natural Sciences and Engineering Research Council (NSERC) of Canada, the Canada Foundation for Innovation (CFI), the British Columbia Knowledge Development Fund (BCKDF), and the University of Victoria for instrumentation and operational funding. K.M. thanks the University of Victoria for a graduate fellowship. F.H. is a Career Scholar of the Michael Smith Foundation for Health Research.

- [1] M. T. Bedford, S. Richard, *Mol. Cell* **2005**, *18*, 263.
- [2] T. C. Osborne, O. Obianyo, X. Zhang, X. Cheng, P. R. Thompson, *Biochemistry* **2007**, *46*, 13370.
- [3] A. Stetler, C. Winograd, J. Sayegh, A. Cheever, E. Patton, X. Zhang, S. Clarke, S. Ceman, *Hum. Mol. Genet.* **2006**, *15*, 87.
- [4] A. J. Bannister, R. Schneider, T. Kouzarides, *Cell* **2002**, *109*, 801.
- [5] Y. Wang, J. Wysocka, J. Sayegh, Y.-H. Lee, J. R. Perlin, L. Leonelli, L. S. Sonbuchner, C. H. McDonald, R. G. Cook, Y. Dou, R. G.

- Roeder, S. Clarke, M. R. Stallcup, C. D. Allis, S. A. Coonrod, *Science* **2004**, *306*, 279.
- [6] J. Murray-Rust, J. Leiper, M. McAlister, J. Phelan, S. Tilley, J. Santa Maria, P. Vallance, N. McDonald, *Nat. Struct. Biol.* **2001**, *8*, 679.
- [7] J. M. Aletta, T. R. Cimato, M. J. Ettinger, *Trends Biochem. Sci.* **1998**, *23*, 89.
- [8] F.-M. Boisvert, U. Dery, J.-Y. Masson, S. Richard, *Genes Dev.* **2005**, *19*, 671.
- [9] F.-M. Boisvert, J. Cote, M.-C. Boulanger, S. Richard, *Mol. Cell. Proteomics* **2003**, *2*, 1319.
- [10] J. Cote, S. Richard, *J. Biol. Chem.* **2005**, *280*, 28476.
- [11] R. M. Hughes, M. L. Waters, *J. Am. Chem. Soc.* **2006**, *128*, 12735.
- [12] P. E. Mason, G. W. Neilson, J. E. Enderby, M. L. Saboungi, C. E. Dempsey, A. D. MacKerell, J. W. Brady, *J. Am. Chem. Soc.* **2004**, *126*, 11462.
- [13] R. D. Mountain, D. Thirumalai, *J. Phys. Chem. A* **2004**, *108*, 19711.
- [14] C. P. G. Butcher, B. F. G. Johnson, J. S. McIndoe, X. Yang, X.-B. Wang, L.-S. Wang, *J. Chem. Phys.* **2002**, *116*, 6560.
- [15] P. J. Dyson, A. K. Hearley, B. F. G. Johnson, J. S. McIndoe, P. R. R. Langridge-Smith, C. Whyte, *Rapid Commun. Mass Spectrom.* **2001**, *15*, 895.
- [16] P. J. Dyson, B. F. G. Johnson, J. S. McIndoe, P. R. R. Langridge-Smith, *Rapid Commun. Mass Spectrom.* **2000**, *14*, 311.
- [17] S. L. G. Husheer, O. Forest, M. Henderson, J. S. McIndoe, *Rapid Commun. Mass Spectrom.* **2005**, *19*, 1352.
- [18] H. Cox, G. Akibo-Betts, R. R. Wright, N. R. Walker, S. Curtis, B. Duncombe, A. J. Stace, *J. Am. Chem. Soc.* **2003**, *125*, 233.
- [19] B. J. Duncombe, K. Duale, A. Buchanan-Smith, A. J. Stace, *J. Phys. Chem. A* **2007**, *111*, 5158.
- [20] N. Toyama, J.-y. Kohno, F. Mafune, T. Kondow, *Chem. Phys. Lett.* **2006**, *419*, 369.
- [21] M. F. Bush, J. S. Prell, R. J. Saykally, E. R. Williams, *J. Am. Chem. Soc.* **2007**, *129*, 13544.
- [22] T. Wyttenbach, D. Liu, M. T. Bowers, *Int. J. Mass Spectrom.* **2005**, *240*, 221.
- [23] F. Vanzi, B. Madan, K. Sharp, *J. Am. Chem. Soc.* **1998**, *120*, 10748.
- [24] S. Boudon, G. Wipff, B. Maignet, *J. Phys. Chem.* **1990**, *94*, 6056.
- [25] S. J. Angyal, W. K. Warburton, *J. Chem. Soc.* **1951**, 2492.
- [26] Spartan '06, *Wavefunction*, Irvine, CA (USA), **2006**.
- [27] S. E. Rodriguez-Cruz, J. S. Klassen, E. R. Williams, *J. Am. Soc. Mass Spectrom.* **1997**, *8*, 565.
- [28] Y. K. Lau, P. Kebarle, *Can. J. Chem.* **1981**, *59*, 151.
- [29] J. S. Klassen, A. T. Blades, P. Kebarle, *J. Phys. Chem.* **1995**, *99*, 15509.
- [30] A. T. Blades, J. S. Klassen, P. Kebarle, *J. Am. Chem. Soc.* **1996**, *118*, 12437.
- [31] S.-W. Lee, P. Freivogel, T. Schindler, J. L. Beauchamp, *J. Am. Chem. Soc.* **1998**, *120*, 11758.
- [32] D. W. Ledman, R. O. Fox, *J. Am. Soc. Mass Spectrom.* **1997**, *8*, 1158.
- [33] S.-W. Lee, H. Cox, W. A. Goddard III, J. L. Beauchamp, *J. Am. Chem. Soc.* **2000**, *122*, 9201.
- [34] A. A. Shvartsburg, K. W. Siu, *J. Am. Chem. Soc.* **2001**, *123*, 10071.
- [35] K. McQuinn, F. Hof, J. S. McIndoe, *Chem. Commun.* **2007**, 4099.
- [36] T. G. Spence, T. D. Burns, L. A. Posey, *J. Phys. Chem. A* **1997**, *101*, 139.
- [37] R. R. Wright, N. R. Walker, S. Firth, A. J. Stace, *J. Phys. Chem. A* **2001**, *105*, 54.
- [38] The difference in height between the contours is simply a result of the manner in which the plots are generated. Only data that has > 4% of the intensity of the largest peak is displayed, and because the intensity of the [Me<sub>6</sub>Guan]<sup>+</sup> peak is so large relative to the other peaks, the contour lines at other hydration values appear to extend over smaller collision voltage ranges.
- [39] M. Meot-Ner, *J. Am. Chem. Soc.* **1983**, *105*, 4912.
- [40] J.-C. Soetens, C. Millot, C. Chipot, G. Jansen, J. G. Angyan, B. Maignet, *J. Phys. Chem. A* **1997**, *101*, 10910.
- [41] P. B. Armentrout, *J. Chem. Phys.* **2007**, *126*, 234302.
- [42] E. Zoicher, R. Sigrist, P. Chen, *Inorg. Chem.* **2007**, *46*, 11366.
- [43] D. R. Carl, R. M. Moision, P. B. Armentrout, *Int. J. Mass Spectrom.* **2007**, *265*, 308.
- [44] J. Schneider, A. Shilatifard, *ACS Chem. Biol.* **2006**, *2*, 75.
- [45] M. G. Lee, R. Villa, P. Trojer, J. Norman, K.-P. Yan, D. Reinberg, L. D. Croce, R. Shiekhattar, *Science* **2007**, *318*, 447.
- [46] A. M. Hogg, R. M. Haynes, P. Kebarle, *J. Am. Chem. Soc.* **1966**, *88*, 28.
- [47] V. N. Nemykin, P. Basu, *Inorg. Chim. Acta* **2005**, *358*, 2876.

Received: January 17, 2008

Published online: June 11, 2008